The Journal of Immunology

Crucial Role of Granulocytic Myeloid-Derived Suppressor Cells in the Regulation of Central Nervous System Autoimmune Disease

Marianna Ioannou, Themis Alissafi, Iakovos Lazaridis, George Deraos, John Matsoukas, Achille Gravanis, Vasileios Mastorodemos, Andreas Plaitakis, Arlene Sharpe, Dimitrios Boumpas and Panayotis Verginis

J Immunol 2012; 188:1136-1146; Prepublished online 30 December 2011;
doi: 10.4049/jimmunol.1101816
http://www.jimmunol.org/content/188/3/1136

The Journal of Immunology is published twice each month by
The American Association of Immunologists, Inc.,
1451 Rockville Pike, Suite 650, Rockville, MD 20852

Print ISSN: 0022-1767 Online ISSN: 1550-6606.

Crucial Role of Granulocytic Myeloid-Derived Suppressor Cells in the Regulation of Central Nervous System Autoimmune Disease

Marianna Ioannou,[*,†] Themis Alissafi,[*,†] Iakovos Lazaridis,[‡] George Deraos,[§] John Matsoukas,[§] Achille Gravanis,[‡] Vasileios Mastorodemos,[¶] Andreas Plaitakis,[¶] Arlene Sharpe,[‖] Dimitrios Boumpas,[*,†] and Panayotis Verginis[*,†]

There is a need in autoimmune diseases to uncover the mechanisms involved in the natural resolution of inflammation. In this article, we demonstrate that granulocytic myeloid-derived suppressor cells (G-MDSCs) abundantly accumulate within the peripheral lymphoid compartments and target organs of mice with experimental autoimmune encephalomyelitis prior to disease remission. In vivo transfer of G-MDSCs ameliorated experimental autoimmune encephalomyelitis, significantly decreased demyelination, and delayed disease onset through inhibition of encephalitogenic Th1 and Th17 immune responses. Exposure of G-MDSCs to the autoimmune milieu led to up-regulation of the programmed death 1 ligand that was required for the G-MDSC–mediated suppressive function both in vitro and in vivo. Importantly, myeloid-derived suppressor cells were enriched in the periphery of subjects with active multiple sclerosis and suppressed the activation and proliferation of autologous CD4$^+$ T cells ex vivo. Collectively, this study revealed a pivotal role for myeloid-derived suppressor cells in the regulation of multiple sclerosis, which could be exploited for therapeutic purposes. *The Journal of Immunology*, **2012, 188: 1136–1146.**

Re-establishment of immune homeostasis and self-tolerance remain unresolved issues in autoimmune inflammatory diseases. Multiple sclerosis (MS) is a chronic inflammatory demyelinating disease of the CNS of unknown etiology (1). Experimental autoimmune encephalomyelitis (EAE) is a well-established animal model that resembles many facets of MS (2) and is used as a tool to study pathogenic, as well as regulatory, processes of the disease. EAE is characterized by periods of exacerbation followed by remission, which mirrors disease course in the majority of MS patients. Disease pathogenesis, progression, and subsequent relapses have been attributed to myelin-reactive Th1 and Th17 cells and their products (3–5). In contrast, several mechanisms involving immune cells, such as CD4$^+$ regulatory T cells (6) and type II monocytes (7) or neutrophils (8), as well as immunosuppressive mediators, like IL-10 (9, 10), have been proposed to regulate EAE both in vivo and in vitro. However, it is poorly understood how inflammation is resolved, disease remits, and, in particular, which immune cells are important for naturally terminating the relapsing phase. Therefore, there is a need to delineate such mechanisms to facilitate the design of more effective protocols for the re-establishment of tolerance and prevention of autoimmune diseases of the CNS.

In recent years, myeloid-derived suppressor cells (MDSCs) have received considerable attention because they potently perturb both innate and adaptive immune responses (11). MDSCs consist of a heterogenous population of myeloid precursors of macrophages, dendritic cells, and granulocytes and are characterized by the coexpression of Gr-1 and CD11b. They can be divided into cells with monocytic or granulocytic morphology, defined as CD11b$^+$ Ly6C$^+$Ly6G$^-$ or CD11b$^+$Ly6C^{low}Ly6G$^+$, respectively (12–14). Extensive studies established a prominent role for MDSCs in the regulation of immune responses in mice during cancer (11, 15, 16), infections (15, 17), and transplantation (18–20); in humans, MDSC accumulation at tumor sites downregulates antitumor immunity, promoting tumor surveillance and growth (21, 22). A variety of mechanisms has been attributed to the MDSC-mediated suppression of immune responses, ranging from cell-to-cell contact to soluble mediators (23, 24). However, it is now appreciated that cells of the myeloid lineage are characterized by increased plasticity, and their functional polarization depends on the local microenvironment (25).

Although the importance of MDSCs in antitumor immunity is well defined, their role in the regulation of autoimmune pathology is just emerging. MDSCs were shown to prevent murine type 1 diabetes (26) and to suppress inflammatory responses in the gut (27), retina (28), and skin (29). The role of MDSCs remains controversial in EAE. Circulating Ly6C$^+$ myeloid precursors were shown to perpetuate disease upon migration to the CNS (30, 31),

*Laboratory of Autoimmunity and Inflammation, University of Crete, Medical School, 71300 Heraklion, Greece; †Institute of Molecular Biology and Biotechnology, Foundation for Research and Technology, 71300 Heraklion, Greece; ‡Department of Pharmacology, University of Crete, Medical School, 71300 Heraklion, Greece; §Department of Chemistry, University of Patras, 26504 Patras, Greece; ¶Department of Neurology, University of Crete Medical School, 71003 Heraklion, Greece; and ‖Department of Pathology, Harvard Medical School, Brigham & Women's Hospital, Boston, MA 02115

Received for publication June 20, 2011. Accepted for publication November 22, 2011.

This work was supported by grants from the European Union's Six Framework (FP6) Autocure project (to P.V. and D.B.) and the Ministry of Development Secretariat of Research and Technology of Greece (Pythagoras I to D.B.). M.I. is supported by a Bodossakis Foundation scholarship.

Address correspondence and reprint requests to Dr. Panayotis Verginis, Laboratory of Autoimmunity and Inflammation, University of Crete Medical School, and Institute of Molecular Biology and Biotechnology, Foundation for Research and Technology, 71300 Heraklion, Greece. E-mail address: verginis@imbb.forth.gr

The online version of this article contains supplemental material.

Abbreviations used in this article: 7AAD, 7-aminoactinomycin D; dLN, draining lymph node; EAE, experimental autoimmune encephalomyelitis; G-MDSC, granulocytic myeloid-derived suppressor cell; LN, lymph node; MDSC, myeloid-derived suppressor cell; M-MDSC, monocytic myeloid-derived suppressor cell; MOG, myelin oligodendrocyte glycoprotein; MS, multiple sclerosis; PD-L, programmed death ligand; PMN, polymorphonuclear cell; ROS, reactive oxygen species; WT, wild-type.

www.jimmunol.org/cgi/doi/10.4049/jimmunol.1101816

whereas other reports demonstrated a regulatory role for MDSCs during EAE (32, 33). Although the increased immunosuppressive properties of MDSCs could make them potential targets for therapeutic intervention of autoimmunity, several questions remain to be addressed. For example, the subset of MDSCs, as well as the precise mechanism exploited by these cells in the modulation of an autoimmune response, is unclear. In addition, the specialized microenvironment that might favor the MDSCs' function needs to be determined. Finally, it remains elusive whether MDSCs have any role in human autoimmune diseases.

In this study, we demonstrate a significant accumulation of $CD11b^{hi}Ly6G^{+}Ly6C^{-}$ granulocytic MDSCs (G-MDSCs) in the spleen of mice with EAE prior to disease resolution. Adoptive transfer of G-MDSCs, isolated from the autoimmune environment, potently suppress the development of EAE and inhibit the priming of autoantigen-specific Th1 and Th17 cells. In addition, G-MDSCs from myelin oligodendrocyte glycoprotein (MOG)-immunized mice express high levels of the coinhibitory molecule programmed death ligand (PD-L)1, which was required to exert their function in vivo. Finally, we demonstrate for the first time, to our knowledge, that MDSCs are significantly increased in the peripheral blood of patients with active MS and are able to suppress the activation and proliferation of autologous T cells in vitro. Together, our data reveal a pivotal role for G-MDSCs in the regulation of CNS autoimmune inflammation.

Materials and Methods

Mice

Female C57BL/6 (B6) mice (6–10 wk) were obtained from the specific pathogen-free facility of the Institute of Molecular Biology and Biotechnology (Heraklion Crete, Greece).

PD-$1^{-/-}$ mice bred on a B6 background were a kind gift of Dr. Zhang (Department of Orthopedic Surgery, University of Chicago, Chicago, IL). PD-$L1^{-/-}$ mice bred on a B6 background (34) were provided by Prof. A. Sharpe (Department of Pathology, Harvard Medical School, Brigham & Women's Hospital). All procedures were in accordance to institutional guidelines and were approved by the Greek Federal Veterinary Office.

Reagents

The following fluorescent-conjugated mAbs were used for analysis of mouse cells. Ly6C (1G7.G10) was from Miltenyi Biotec, and Gr-1 (RB6-8C5), CD80 (16-10A1), CD86 (PO3.1), CD40 (1C10), CD273 (PD-L2, 122), Foxp3 (FJK-16s), and IgG1k isotype control (P3) were from eBioscience. CD11b (M1/70), CD3e (145-2C11), CD19 (1D3), CD274 (PD-L1, M1H5), CD45R/B220 (RA3-6B2), CD4 (RM4-5), Ly6G (1A8), CD44 (Pgp-1, Ly24), I-A^{b} (AF6-120.1), and CD25 (PC61) were from BD Pharmingen.

The following mAbs were used for human cell phenotypes. CD15 (8OH5), CD33 (D3HL60.251), CD14 (RM052), and CD25 (B1.49.9) were from Beckman Coulter. HLA-DR (L243, G46-6) and CD4 (RPA-T4) were from BD Pharmingen. B7-H1 (PD-L1) (MIH1) was from eBioscience. Anti-human PD-L1 mAb (IgG2b, 29E.2A3) was kindly provided by Prof. G. Freeman (Department of Medicine, Harvard Medical School and Dana Farber Cancer Institute, Boston, MA). Mouse IgG2b isotype control was from Sigma.

PE-conjugated $MOG_{38–49}/IA^{b}$ (MHC class II)-specific tetramer and hCLIP/IA^{b} control tetramer were obtained from the National Institutes of Heath tetramer facility.

Cell cultures were performed in DMEM or RPMI 1640, both supplemented with 10% FBS, penicillin (100 U/ml), streptomycin (100 μg/ml), and 2-ME (5×10^{-5} M) all from Life Technologies (Carlsbad, CA). Recombinant mouse IFN-γ and IL-4 were purchased from PeproTech, *Escherichia coli* LPS was from InvivoGen, and PMA was from Sigma-Aldrich.

$MOG_{35–55}$ peptide [MEVGWYRSPFSRVVHLYRNGK] was synthesized by the Department of Chemistry, University of Patras, and was purified to >95% by HPLC.

EAE induction and adoptive-transfer experiments

EAE was induced in mice by immunization with 100 μg $MOG_{35–55}$ peptide emulsified in CFA (Sigma) s.c. at the base of the tail and i.p. injections of 200 ng pertussis toxin (Sigma) at the time of immunization and 48 h later. For adoptive-transfer experiments, 7-aminoactinomycin D $(7AAD)^{-}CD3^{-}CD19^{-}$ $CD11b^{hi}Ly6G^{+}$ (G-MDSCs) or $Ly6G^{-}CD11b^{+}$ $(7AAD^{-}CD3^{-}CD19^{-})$ cells were sorted (purity > 95%) from spleens of MOG/CFA-immunized mice and transferred (2×10^{6} cells) i.v. into syngeneic hosts (two donors/one recipient), as indicated. In some experiments, sorted G-MDSCs from PD-$L1^{-/-}$ MOG/CFA-immunized mice were used. Mice were monitored daily for clinical signs of disease. Clinical scores of EAE were assessed as follows: 0, no disease; 1, limp tail; 2, hind limp weakness; 3, hind limb paralysis; 4, hind limb and forelimb paralysis; and 5, moribund state.

Immunofluorescence and histology

Mice were deeply anesthetized with sodium pentobarbital (Dolethal, 0.7 ml/kg, i.p.), perfused transcardially with heparinized saline solution for ~15 min, and then perfused with 4% paraformaldehyde, 15% picric acid, and 0.05% glutaraldehyde in phosphate buffer 0.1 M. Spinal cords of perfused mice were collected and maintained in the same fixative overnight at 4°C. Spinal cords were embedded in 2.5% agarose and stored at 4°C in 0.1 M phosphate buffer. The samples were sectioned (45 μm, longitudinally) in a vibratome, and free-floating sections were processed for immunostaining with anti-MBP 1:500 (ab980; Chemicon), anti-CD11b 1:100 (BD 55330), or anti–Ly-6G 1:100 (BD 551459), followed by incubation with secondary Abs (Alexa Fluor 488, 546, and 633; 1:1000 in TBST 0.1%). Then samples were coverslipped with VECTASHIELD (Vector, H-1400) and visualized using a confocal microscope. For MBP staining, sections were also counterstained with Hoechst fluorescent dye. For histology, mice were perfused with 10% neutral-buffered formalin. The spinal cords were dissected out, fixed in the same fixative, and embedded in paraffin. Transverse sections (6–7 μm) from cervical, thoracic, and lumbar regions were stained with H&E for histological analysis using a Nikon Eclipse E800 microscope.

Flow cytometry and cell sorting

Cells were stained for extracellular markers for 20 min at 4°C in PBS/5% FCS. Intracellular Foxp3 staining was performed using the anti-mouse Foxp3 staining set, according to the manufacturer's protocol (eBioscience). Dead cells were identified and excluded from all analyses by 7AAD (BD Pharmingen). For tetramer staining, lymph node (LN) cells (2×10^{6} cells) were incubated for 5 min with 10% mouse and rat sera (Jackson ImmunoResearch Laboratories), followed by a 45-min staining with 10 μg/ml tetramer at room temperature. mAbs and viability dyes were subsequently added for 20 min on ice. Cells were acquired on a FACSCalibur (BD Biosciences) and analyzed using FlowJo software (Tree Star). Cell sorting was performed using the high-speed cell sorter MoFlo (Dako).

T cell-proliferation assays and cytokine assessment

Draining inguinal LNs were harvested 9–10 d after immunization and were cultured (6×10^{5} cells/200 μl/well) in the presence or absence of $MOG_{35–55}$ peptide for 72 h. Cells were then pulsed with 1 μCi ^{3}[H] thymidine (TRK120; Amersham Biosciences) for 18 h, and incorporated radioactivity was measured using a Beckman β counter. Results are expressed as stimulation index, which is defined as cpm in the presence of Ag/cpm in the absence of Ag. Cytokines were assessed in culture supernatants collected after 48 h of stimulation. Detection of IL-2, IFN-γ (BD OptEIA; BD Biosciences), and IL-17 (R&D Systems) was performed by ELISA, following the manufacturer's recommendations. Light absorbance at 450 nm was measured using a Vmax plate reader (Bio-Rad). In other experiments, inguinal LNs were dissected and analyzed by flow cytometry, as indicated in the figure legends.

MS subjects

MS patients were recruited through the Neurology Department, University Hospital of Heraklion (Crete, Greece). The disease's diagnosis and classification were established by the clinical and magnetic resonance imaging criteria of the International Panel on MS. Other autoimmune and/or immune-mediated or infectious diseases of the CNS were sought out and excluded by appropriate clinical and diagnostic evaluations. MS subjects with active disease were those with acute or subacute neurologic symptoms either due to the initial MS episode (disease onset) or to a subsequent relapse, followed by improvement. In contrast, patients with relapsing-remitting MS who were clinically stable and who had experienced no clinical exacerbation for ≥6 mo prior to the time of the study were considered to be in remission. The Clinical Research Ethics Board at the University Hospital of Crete (Heraklion, Crete) approved this study. Informed consent was obtained from all patients prior to sample collection.

Human cell isolation from peripheral blood

Heparinized blood was collected from healthy subjects and MS patients, and PBMCs were isolated on Histopaque-1077 (Sigma) density gradient. MDSCs and $CD4^+$ T cells were analyzed by flow cytometry and sorted as described. The Clinical Research Ethics Board at the University Hospital of Crete (Heraklion, Crete) approved this study.

In vitro-suppression assay

Naive mouse $CD4^+CD25^-$ T cells (from B6 or $PD1^{-/-}$ mice) were sorted (purity > 99%) and were stimulated with 10 μg/ml plate-bound anti-CD3 (145-2C11; BD Pharmingen) and 1 μg/ml anti-CD28 (37.51; BD Pharmingen). Purified $CD11b^+Ly6G^+$ MDSCs (purity > 95%) were activated with recombinant mouse IFN-γ for 24 h and then added to the culture at a 1:1 ratio. Proliferation was assessed by $[^3H]$thymidine uptake.

Human $CD4^+CD25^-$ T cells were sorted (purity > 99%) from PBMCs, labeled with CFSE (1 μM for 10 min at 37°C in labeling buffer-PBS/0.1% BSA), and cocultured (2×10^4 cells/well) with sorted MDSCs (purity > 95%), at a 1:1 ratio, in the presence of 2 μg/ml plate bound anti-CD3 (OKT3; e-Bioscience) and 1 μg/ml anti-CD28 (CD28.2; e-Bioscience). Proliferation of T cells was determined based on CFSE dilution by flow cytometry. The levels of IL-2 in culture supernatants were measured after 48 h using a human cytokine ELISA kit (eBioscience).

Phenotypic analysis

Sorted G-MDSCs or $Ly6G^-CD11b^+$ ($7AAD^-CD3^-CD19^-$) cells were cultured (1.5×10^6 cells/ml) in the presence of recombinant mouse IFN-γ (20 ng/ml), LPS (1 μg/ml), or IL-4 (20 ng/ml) for 18–20 h. Cell surface markers were assessed by flow cytometry. Nitrite quantification was assayed using the Greiss reagent system (Promega), following the manufacturer's instructions. Bone marrow-derived macrophages generated in the presence of L929 cell-conditioned medium containing M-CSF and activated with LPS (1 μg/ml) for 12 h were used as a positive control. Cultured supernatants were assessed for production of IL-10 and IL-12 by ELISA (BD OptEIA; BD Biosciences). Arginase I production was determined by Western blot analysis. Briefly, whole-cell lysates (40 μg protein) were subjected to SDS-PAGE electrophoresis on 10% gels and then transferred to nitrocellulose membranes (Protran; Whatman). Membranes were blocked with 5% milk in TBST and then incubated with anti-arginase I Ab (1:1000; BD Biosciences), as well as anti–β-tubulin (1:2000; Sigma) as a loading control. Detection was performed using HRP-conjugated anti-Ig (Sigma) and chemiluminescent reagents (Supersignal Substrate; Pierce). Reactive oxygen species (ROS) production was determined using the oxidation-sensitive dye aminophenyl fluorescein (Cell Technology) by flow cytometry.

PBMCs from healthy individuals or active MS patients were cultured in the presence of recombinant human IFN-γ (20 ng/ml; PeproTech) and analyzed for PD-L1 expression.

Morphologic analysis

G-MDSCs or monocytic MDSCs (M-MDSCs), sorted from spleens of MOG/CFA-immunized mice, or $HLA\text{-}DR^{-/low}CD14^-CD15^+CD33^+$ cells, sorted from PBMCs of active MS patients, were collected on precoated (poly-L-lysine) coverslips, fixed with methanol, and stained with May–Grunwald and Giemsa dye for 5 and 10 min, respectively. Images were obtained using the Nikon Eclipse E800 microscope.

Preparation of CNS mononuclear cells

Spinal cords dissected from PBS-perfused mice and mononuclear cells were isolated by passing the tissue through a cell strainer (70 μm), followed by a Percoll-gradient (70%/30%) centrifugation. Mononuclear cells were removed from the interphase, washed, and resuspended in culture medium for further analysis.

Statistics

The *p* values were derived using two-tailed Student *t* tests, when indicated. The Mann–Whitney *U* test was used for the statistical analysis of human MDSC frequency. The nonparametric Wilcoxon signed-rank test was used in the longitudinal analysis of MDSCs in MS patients. All analyses were performed using Prism (GraphPad Software).

Results

Increased accumulation of G-MDSCs at the peripheral lymphoid compartments of mice with EAE

We first determined the kinetics of $CD11b^+Gr1^+$ MDSC expansion and/or accumulation in the peripheral lymphoid organs during the different phases of $MOG_{35–55}$-induced EAE (Fig. 1*A*). The frequency of $CD11b^+Gr1^+$ MDSCs ($7AAD^-CD3^-CD19^-$) increased during the asymptomatic phase and even more so at the onset of disease, reached the maximum at the peak of EAE, prior to disease remission, and contracted upon resolution of disease (Fig. 1*B*). Among the two subsets of MDSCs, only granulocytic-like cells ($7AAD^-CD3^-CD19^-CD11b^{hi}Ly6G^+Ly6C^-$ cells) closely followed the kinetics of EAE, because their frequency (Fig. 1*C*) and absolute numbers (Fig. 1*D*) gradually increased until disease peak and declined at the recovery phase, reaching basal levels at disease resolution. In contrast, the frequency (Fig. 1*C*) and absolute numbers (Fig. 1*D*) of $7AAD^-CD3^-CD19^-CD11b^{hi}Ly6C^+$ MDSCs were not significantly altered during the course of EAE. Morphological analysis of sorted $7AAD^-CD3^-CD19^-CD11b^{hi}Ly6G^+$ MDSCs (G-MDSCs) from spleens of MOG/CFA-immunized mice revealed ring-shaped multilobed nuclei, consistent with the granulocytic origin of this MDSC subset, whereas $7AAD^-CD3^-CD19^-CD11b^{hi}Ly6C^+$ MDSCs showed a monocytic morphology, indicating that they were M-MDSCs (Fig. 1*E*). Notably, flow cytometry analysis revealed increased frequency of G-MDSCs in the spinal cord infiltrates isolated from mice during the peak of EAE (Fig. 1*F*), as well as the draining cervical LNs (Supplemental Fig. 1). Consistent with the flow cytometry data, immunofluorescent analysis of spinal cords demonstrated specific localization of $CD11b^+Ly6G^+$ MDSCs among the inflammatory infiltrates (Fig. 1*G*). Collectively, our data showed an increased accumulation of G-MDSCs in CNS and enhanced recruitment of this subset at lymphoid organs peaking prior to resolution of EAE. Together, these findings raised the possibility of an MDSC-mediated role in the resolution of the autoimmune response.

Adoptive transfer of G-MDSCs ameliorates $MOG_{35–55}$-induced EAE

To examine the ability of G-MDSCs to mediate disease remission, we adoptively transferred purified G-MDSCs isolated from spleens of MOG/CFA-immunized mice into recipient mice during the course of EAE (Fig. 2*A*). $Ly6G^-CD11b^+$ myeloid cells isolated from the same mice were used as controls. Adoptive transfer of G-MDSCs decreased the severity of EAE (Fig. 2*B*) compared with either untreated group (**$p = 0.0056$ at day 14 after the antigenic challenge) or $Ly6G^-CD11b^+$-treated mice (**$p = 0.0047$ at day 14 after the antigenic challenge), as well as significantly delayed disease onset (Fig. 2*B*, 2*C*). Disease amelioration in G-MDSC–treated mice was accompanied with reduced inflammatory lesions in the spinal cords (Fig. 2*D*) and diminished demyelination (Fig. 2*E*) compared with control groups. The few inflammatory foci detected in G-MDSC–treated mice were mostly located at the meningeal regions, with little or no parenchymal infiltration. Importantly, immunofluorescent analysis showed increased accumulation of $CD11b^+Ly6G^+$ MDSCs at the inflammatory lesion in the meningeal area of spinal cord of G-MDSC–treated mice, whereas this was not the case in the other two groups of mice (Fig. 2*F*). Collectively, these results indicated that G-MDSCs potently suppress the clinical and pathologic features of EAE.

G-MDSCs suppress the priming of $MOG_{35–55}$-specific Th1 and Th17 cells in vivo

Because EAE is initiated and perpetuated by autoreactive Th1 and Th17 cells, we further assessed whether in vivo transfer of G-MDSCs could influence the priming of MOG-specific T cells in the peripheral LNs. To address this, mice were adoptively transferred with G-MDSCs as described in Fig 2*A*; 9 d after the antigenic challenge, inguinal draining LNs (dLNs) were assessed for $MOG_{35–55}$-specific T cell responses. We noted that G-MDSC

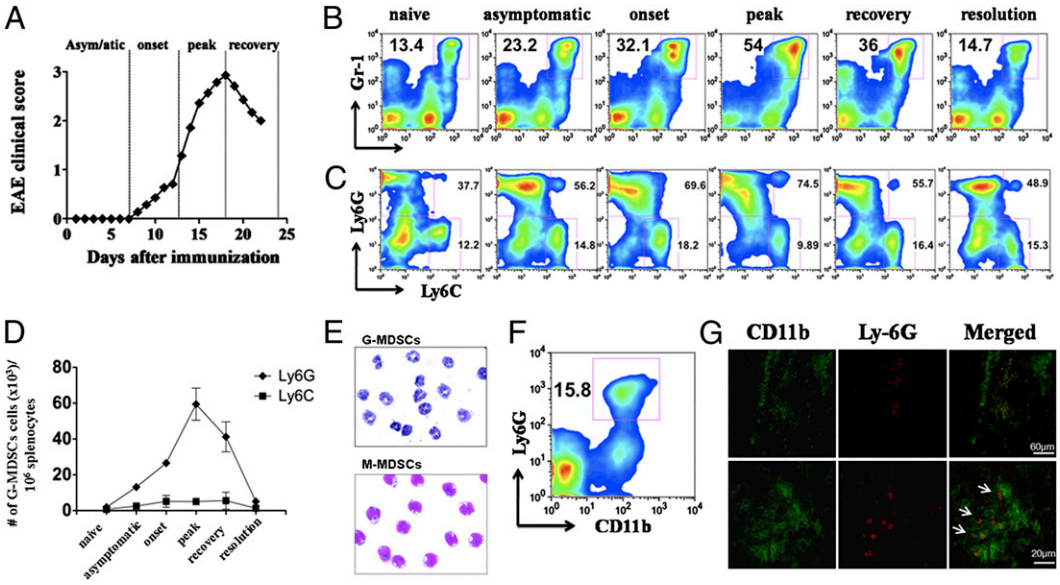

FIGURE 1. Recruitment of granulocytic Ly6G$^+$ MDSCs in the peripheral lymphoid organs correlates with disease activity in EAE. *A*, $MOG_{35–55}$-induced EAE in C57BL/6 mice. Mean clinical score is shown (n = 7). Kinetics of CD11b$^+$Gr1$^+$ MDSC (*B*) and G-MDSC (*C*) accumulation in the spleen of mice during the different phases of EAE. Representative flow cytometric analysis indicates percentages of MDSCs. Gates were set on 7AAD$^-$CD3$^-$CD19$^-$ or 7AAD$^-$CD3$^-$CD19$^-$CD11b^{hi} cells for *B* and *C*, respectively. *D*, Relative numbers of Ly6G$^+$ MDSCs and Ly6C$^+$ MDSCs/10^6 splenocytes during the different phases of EAE (mean ± SD of four mice/time point). *E*, Morphological analysis of G-MDSCs and M-MDSCs, sorted from spleens of MOG/CFA-primed mice, using May–Grunwald–Giemsa staining. *F*, Frequency of G-MDSCs in the spinal cords of mice at the peak of EAE. Gates were set on 7AAD$^-$CD3$^-$CD19$^-$ cells. Data are representative of four or five separate experiments. *G*, Immunofluorescence staining for CD11b (green) and Ly6G (red) in spinal cord sections at disease peak (score 3, 5). Arrows show CD11b$^+$Ly6G$^+$ infiltrating cells. Original magnification ×40 and ×60 1,65. Sections are representative of three mice analyzed individually.

transfer resulted in decreased frequency (Fig. 3*A*) and significantly reduced numbers (Fig. 3*B*) of $MOG_{38–49}$/IA^{b+}CD3$^+$CD4$^+$ T cells compared with control untreated mice, indicating that G-MDSCs suppressed the expansion of autoreactive T cells. This was confirmed upon ex vivo stimulation of dLNs with MOG peptide; LNs from G-MDSC–treated mice showed markedly reduced cell proliferation and significant suppression of Th1- and Th-17–secreting cytokines compared with the untreated control group (Fig. 3*C*). Suppression of MOG-specific Th1 and Th17 responses was accompanied by increased accumulation of G-MDSCs in the dLNs of G-MDSC–injected mice compared with the control group (Fig. 3*D*). In contrast, no significant difference in the frequency of CD4$^+$Foxp3$^+$ regulatory T cells was observed (Fig. 3*E*). Collectively, these results demonstrated the suppressogenic potential of G-MDSCs against MOG-specific autoreactive T cells in vivo.

Phenotypic characterization of G-MDSCs in MOG/CFA-immunized mice

Several mechanisms of suppression have been assigned to MDSCs during cancer and infection (11, 35). However, it remains to be determined how G-MDSCs exert their function in an autoimmune setting. To address this, G-MDSCs were sorted from MOG/CFA-immunized mice and treated for 24 h with LPS or IFN-γ, two well-known proinflammatory stimuli. Assessment of cytokines in culture supernatants showed increased secretion of IL-10 upon LPS or LPS/IFN-γ stimulation (Fig. 4*A*), whereas IL-12 was not detected (Fig. 4*B*). In addition, neither NO (Fig. 4*C*) nor Arg-1 (Fig. 4*D*) could be detected in stimulated G-MDSCs, whereas intracellular ROS accumulation was only observed upon PMA treatment (Fig. 4*E*). In contrast, detailed cell surface phenotypic analysis of untreated G-MDSCs revealed an increased expression of the inhibitory molecule PD-L1 (Fig. 4*F*). Interestingly, treatment with LPS caused a significant up-regulation of PD-L1 expression, which was even more robust in IFN-γ–treated G-MDSCs (Fig. 4*F*). Enhanced expression of PD-L1 on G-MDSCs upon treatment with IFN-γ was specific, because expression of other costimulatory/inhibitory markers, such as CD80, CD86, CD40, and PD-L2, was not altered (Fig. 4*F*).

PD-L1 is required for G-MDSC–mediated suppression of EAE

PD-L1/PD-1 interactions were reported to deliver coinhibitory signals leading to attenuation of T cell responses both in vitro and in vivo (34, 36). To test the functional significance of the increased PD-L1 expression observed in G-MDSCs, we first compared the activation and proliferation of naive CD4$^+$CD25$^-$ T cells isolated from wild-type (WT) versus PD-1 knockout (PD-1$^{-/-}$) mice in the presence or absence of IFN-γ–treated G-MDSCs (Fig. 5*A*). To this end, the presence of G-MDSCs significantly reduced the frequency of CD4$^+$CD44^{hi} activated WT T cells, whereas the activation of PD-1$^{-/-}$ T cells was not affected (Fig. 5*B*). Moreover, G-MDSCs significantly inhibited WT T cell proliferation, whereas PD-1$^{-/-}$ T cells were resistant to G-MDSC–mediated suppression (Fig. 5*C*). Overall, these data indicated that IFN-γ–exposed G-MDSCs suppressed T cell responses via the PD-1/PD-L1 inhibitory pathway in vitro. To examine whether PD-L1 expression by G-MDSCs confers a dominant mechanism of EAE suppression, we adoptively transferred G-MDSCs isolated from MOG/CFA-immunized PD-L1$^{-/-}$ mice into syngeneic recipients during the course of EAE, as described in Fig. 2*A*. Deficiency of PD-L1 on G-MDSCs abrogated their suppressive ability, because the disease onset and severity were not significantly different between treated and control mice (Fig. 5*D*). This finding correlated with immunohistological analysis of the spinal cords of the two groups of mice, for which a comparable degree of demyelination was observed (Fig. 5*E*). Moreover, analysis of the dLNs of PD-L1$^{-/-}$ G-MDSC–treated mice showed a comparable frequency of $MOG_{38–49}$/IA^{b+}CD3$^+$CD4$^+$ effector T cells as in untreated mice (Fig. 5*F*). Collectively, these data provided direct

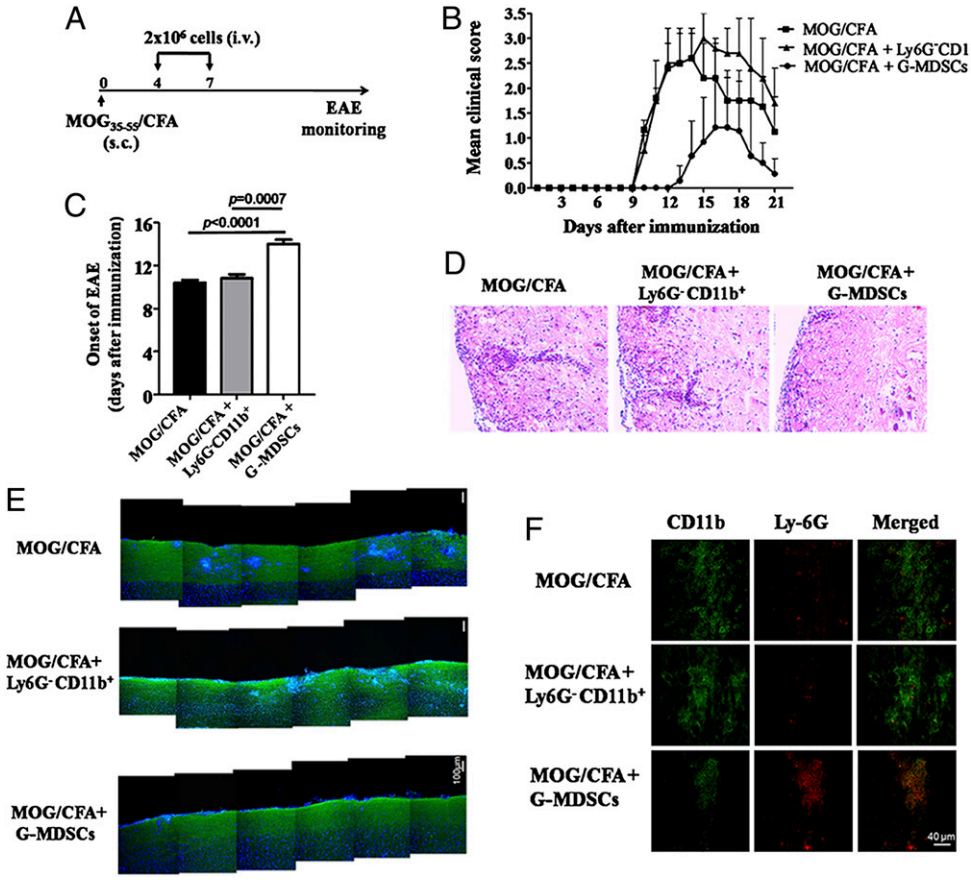

FIGURE 2. Adoptive transfer of G-MDSCs suppresses the clinical course of EAE. *A*, G-MDSCs or Ly6G$^-$CD11b$^+$ cells were sorted from spleens of MOG/CFA-immunized mice (purity > 95%) and adoptively transferred (2×10^6/mouse) into syngeneic MOG/CFA-treated recipients on days 4 and 7 after antigenic challenge. *B*, Mean clinical score of EAE (± SD) in treated or control mice ($n = 7$ mice/group). *C*, EAE onset in indicated groups of mice (mean ± SD; p values were calculated using the t test). *D–F*, Immunohistological analysis of spinal cords isolated from the indicated groups of mice 12–14 d after antigenic challenge. *D*, H&E staining. *E*, MBP (green) and Hoechst (blue). *F*, CD11b (green), Ly6G (red), and two-color overlay (original magnification ×60). Results are representative of two or three independent experiments.

evidence for a PD-L1–dependent G-MDSC–mediated suppression of the autoimmune response.

Human G-MDSCs from MS patients potently suppress the activation and proliferation of autologous T cells in vitro

We next examined the presence of MDSCs in MS subjects in the active phase of disease or during remission. Human MDSCs have mainly been studied in cancer patients and are characterized as HLA-DR$^{-/low}$CD14$^-$CD33$^+$CD15$^+$ (37, 38). Flow cytometry analysis revealed significantly increased frequency (Fig. 6*A*) and numbers (Fig. 6*B*) of HLA-DR$^{-/low}$CD14$^-$CD33$^+$CD15$^+$ MDSCs in the peripheral blood of patients with active MS compared with patients in remission or healthy controls. A significant decrease in MDSC numbers was also observed upon longitudinal analysis of CD33$^+$CD15$^+$ cells in seven active MS patients who achieved remission (Fig. 6*C*). Similar to mouse G-MDSCs, morphologic analysis of sorted HLA-DR$^{-/low}$CD14$^-$CD33$^+$CD15$^+$ cells from active MS patients showed cells with a multilobed nucleus consistent with a granulocytic phenotype (Fig. 6*D*). We next assessed the ability of CD33$^+$CD15$^+$ MDSCs to suppress the activation and proliferation of stimulated autologous CD4$^+$CD25$^-$ cells. To this end, sorted highly pure human MDSCs (CD33$^+$CD15$^+$HLA-DR$^{-/low}$ CD14$^-$, purity > 95%) from active MS patients were cocultured with autologous sorted CFSE-labeled CD4$^+$CD25$^-$ responder T cells (purity > 98%) stimulated with anti-CD3/CD28. After 5 d of coculture, human MDSCs potently inhibited the activation of responder T cells, as indicated by CD25 expression (Fig. 7*A*). Importantly, although responder T cells underwent at least three or four cell divisions (1st, 24.4%; 2nd, 7.52%; 3rd, 3.06), as traced by the dilution of CFSE, the presence of MDSCs in the culture caused a proliferation arrest of responder T cells to only one or two cell divisions (1st, 15.4%; 2nd, 5.82%) after 5 d of culture (Fig. 7*B*). MDSC-mediated suppression of T cell proliferation was significant, as extrapolated by enumeration of the CD4$^+$ T cells following the 5-d coculture (Fig. 7*C*). This was further supported by a significant reduction in IL-2 secretion in supernatants of MDSCs/CD4$^+$CD25$^-$ cocultures compared with control cultures (Fig. 7*D*). The reduced CD25 expression and T cell proliferation was not due to unspecific blocking effects of the CD33$^+$CD15$^+$ cells, because culture of T cells with autologous CD14$^+$ monocytes increased T cell proliferation and CD25 expression (Supplemental Fig. 2). To examine whether PD-L1 was expressed by the CD33$^+$CD15$^+$ MDSCs, we performed flow cytometry analysis on freshly purified PBMCs. Our data demonstrated an increased expression of PD-L1 in CD33$^+$CD15$^+$ cells from MS patients compared with cells from healthy individuals (Fig. 7*E*, *left panel*). Moreover, treatment of PBMCs from active MS patients for 24 h resulted in up-regulation of PD-L1 (Fig. 7*E*, *right panel*), suggesting that PD-L1 might be involved in MDSC-mediated suppression. To address this, we set up coculture experiments, as described above, in the presence or absence of blocking anti-human PD-L1 mAb. A shown in Fig. 7*F*, blocking of PD-L1 was able to partially block the inhibitory potential of CD33$^+$ CD15$^+$ cells but not completely restore the proliferative ability of

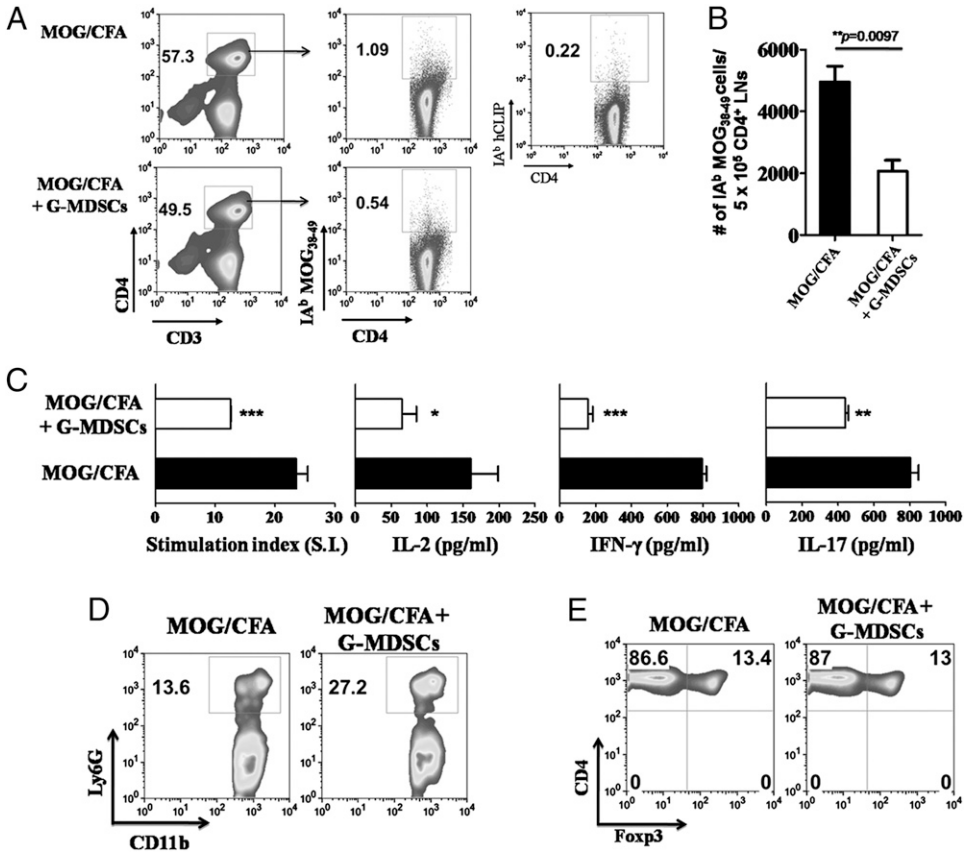

FIGURE 3. G-MDSCs suppress myelin-specific Th1- and Th17-mediated immune responses in the draining LNs. *A*, MOG/CFA-immunized mice were adoptively transferred with G-MDSCs, as in Fig. 2*A*. Inguinal LNs were isolated 9 d after the antigenic challenge and assayed for tetramer binding on $7AAD^-B220^-CD8^-CD3^+CD4^+$ cells. Staining with IA^b-hCLIP tetramer on LNs from MOG/CFA-immunized animals was performed and used as a negative control. Numbers denotes frequency of $CD4^+CD3^+$ cells (*left panels*) and $MOG_{38-49}/IA^{b+}/CD4^+$ cells (*right panel*). *B*, Relative numbers of MOG_{38-49}/IA^{b+} cells/5×10^5 $CD4^+$ LNs (mean ± SD; *p* value, *t* test). *C*, LNs were restimulated in vitro with MOG_{35-55} (15 μg/ml) for 72 h, followed by [^{3}H]thymidine pulsing for 18 h. Incorporated thymidine was measured, and cell proliferation is expressed as stimulation index (*far left panel*). Mean ± SD of triplicate wells. ***$p = 0.0002$, *t* test. Culture supernatants were collected after 48 h of culture and assessed for the presence of IL-2 (*middle left panel*), IFN-γ (*middle right panel*), and IL-17 (*far right panel*) by ELISA. *$p = 0.01$, **$p = 0.002$, ***$p = 0.0003$, *t* test. *D*, Frequency of G-MDSCs in the dLNs of treated and control mice. Gates were set as in Fig. 1*C*, and numbers represent percentages. *E*, Dot plots show percentages of $CD4^+Foxp3^+$ ($7AAD^-B220^-CD3^+$) cells in the LNs of the two groups of mice. Data are derived from two independent experiments with three or four mice/group. Each mouse was analyzed individually.

$CD4^+CD25^-$ autologous T cells. These results demonstrated that PD-L1 expression by human $CD33^+CD15^+$ MDSCs might be involved in MDSC-mediated suppression and indicated that other mediators have to participate, because blocking of PD-L1 does not fully restore human T cell proliferation. Overall, our results demonstrated a significant enrichment of G-MDSCs in active MS patients with a potent ability to suppress the activation and expansion of autologous T cells.

Discussion

Resolution of inflammation during the course of an autoimmune disease is governed by diverse and complex mechanisms likely acting in concert. A comprehensive understanding of the cellular and soluble mediators should facilitate the design of more specialized therapeutic protocols. In this article, we provide compelling evidence for a pivotal role for granulocytic $CD11b^{hi}Ly6G^+$ MDSCs (G-MDSCs) in the regulation of CNS autoimmune inflammation. Thus, in vivo transfer of highly purified G-MDSCs ameliorated EAE, significantly reduced the expansion of autoreactive T cells in the dLNs, and constrained pathogenic Th1 and Th17 immune responses in a PD-L1/IFN-γ–dependent fashion. Importantly, our results demonstrate for the first time, to our knowledge, an important role for G-MDSCs in patients with MS, because this subset was significantly increased in the periphery during active disease and potently suppressed autologous T cell proliferation in vitro. Together, these data highlight the potential of G-MDSCs to serve as a novel target for pharmacologic intervention in autoimmune inflammatory diseases.

It is not clear whether the G-MDSCs described in this article represent a subset of neutrophils or are undifferentiated myeloid suppressor cells. G-MDSCs isolated from MOG/CFA-immunized mice had a high side scatter profile and phenotypically displayed features of neutrophils, such as multilobed nucleus and expression of the typical marker Ly6G. Mounting evidence suggests that, similar to macrophages, polymorphonuclear cells (PMNs) are versatile cells and could acquire diverse functions depending upon the microenvironment. Thus, in the malignancy setting, tumor-associated neutrophils were polarized into either an antitumorigenic (N1) or a protumorigenic (N2) population, depending upon the tumor milieu (39). Moreover, in a systemic inflammatory model, two operationally different PMN populations were characterized: PMN-I and PMN-II, which produced high levels of IL-12 and IL-10, respectively (40). Similarly, in an infectious disease setting, mycobacteria-exposed neutrophils secreted high levels of IL-10, thus possessing anti-inflammatory properties (41). We found that, in the autoimmune environment generated by the in-

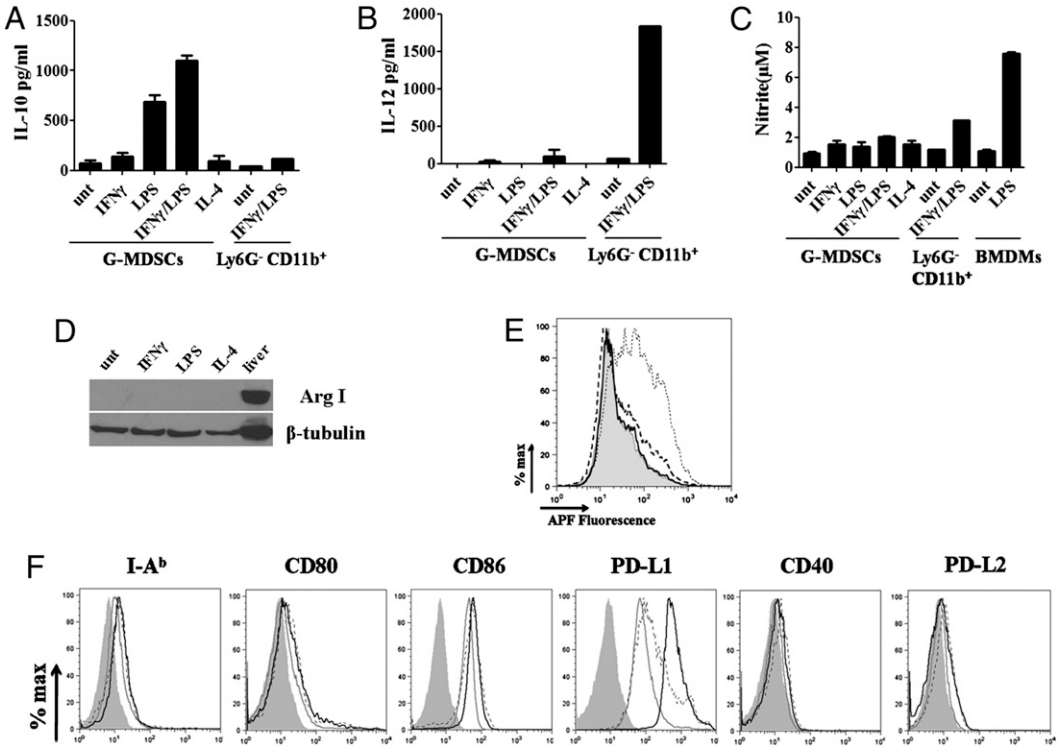

FIGURE 4. Phenotypic characterization of G-MDSCs isolated from MOG/CFA-immunized mice. Sorted G-MDSCs or Ly6G$^-$ CD11b$^+$ cells from spleens of MOG/CFA-primed mice were cultured in the presence of IFN-γ (20 ng/ml), LPS (1 μg/ml), or IL-4 (20 ng/ml) for 18–20 h, and supernatants were assessed for IL-10 (*A*), IL-12 (*B*), and NO (*C*) production (mean ± SD). When indicated, bone marrow-derived macrophages (BMDMs) were used as positive controls. *D*, Western-blot analysis of arginase I (Arg I) expression in G-MDSCs isolated and treated as described above. Whole-cell lysate from liver was used as a positive control. *E*, G-MDSCs, isolated as above, were stimulated for 1 h in the presence of IFN-γ (20 ng/ml), LPS (1 μg/ml), or PMA (5 ng/ml), followed by addition of 10 μM aminophenyl fluorescein. Detection of intracellular ROS accumulation was determined by flow cytometry. Shaded, solid, dashed, and dotted graphs represent untreated or IFN-γ–, LPS-, or PMA-treated cells, respectively. Representative experiment from a total of three is shown. *F*, Expression of the indicated cell surface molecules on G-MDSCs (7AAD$^-$CD3$^-$CD19$^-$CD11b^{hi}, >95% purity) was performed by flow cytometry. G-MDSCs were cultured for 24 h in the presence of IFN-γ (20 ng/ml; solid line) or LPS (1 μg/ml; dashed line). Shaded graphs show isotype-matched mAb-stained cells, and open graphs represent untreated cells. Data are representative of four independent experiments.

jection of a self-Ag in adjuvant, G-MDSCs secreted elevated levels of IL-10 but not IL-12, a profile consistent with the PMN-II regulatory cells characterized above. Irrespective of the differentiation status of G-MDSCs in the autoimmune setting, our data undoubtedly established a regulatory role for granulocytic "neutrophil"-like myeloid cells in the resolution of autoimmune inflammation. Further phenotypic characterization of the regulatory granulocytic cells and development of genetic approaches for the specific depletion of the polarized PMN subsets are needed to reassess their potential in the regulation of immune responses.

Our work provides evidence for a G-MDSC regulation of EAE at the target tissue. Thus, upon adoptive transfer of G-MDSCs in MOG/CFA-immunized mice, we observed reduced inflammation and demyelination in the spinal cord. This, in turn, correlated with delayed disease onset and amelioration of clinical symptoms. Importantly, we also observed an increased accumulation of G-MDSCs at the meningeal lesions of spinal cord, suggesting that G-MDSCs could exert their function at the peripheral lymphoid organs, as well as at the target tissue. This is in agreement with recent data demonstrating that MDSCs suppress preferentially at the inflammatory site in a mouse model of prostate cancer (42). It remains to be determined whether G-MDSCs within the spinal cord during the natural course of the disease possess an inflammatory or anti-inflammatory role. The mechanism involved in G-MDSC trafficking, migration, and specific localization is unknown. One possibility is that proinflammatory cytokines, such as IL-1β (43–45), and chemokines produced during the early infiltration of immune cells into the tissue could direct the extravasation of G-MDSCs. Alternatively, products of Th1 and/or Th17 cells infiltrated into the CNS could mediate such a process. For example, IL-17 was implicated in granulocyte recruitment during inflammatory responses (46). Finally, T cell Ig and mucin domain 3 expressed on Th1 cells was recently reported to facilitate G-MDSC recruitment through binding to galectin-9 (32). Further investigation of the molecules and/or growth factors involved in the specific trafficking of G-MDSCs at inflammatory sites is needed.

Although the function of MDSCs in a malignant disease environment has been addressed (24), the mechanisms underlying their suppressive activity in an autoimmune setting have not been explored. In our experiments, G-MDSCs isolated from MOG/CFA-immunized mice and exposed to IFN-γ in vitro failed to express NO, Arginase I, or ROS, which have been closely linked to MDSC-mediated suppression of antitumor immunity. These findings suggested that the autoimmune environment might induce a novel regulatory signature on G-MDSCs. Indeed, further characterization revealed a significant IFN-γ–mediated up-regulation of the inhibitory molecule PD-L1. Thus, adoptive transfer of PD-L1–deficient G-MDSCs during the course of EAE failed to suppress disease pathology and to limit the expansion of encephalitogenic T cells in the dLNs. Published data established a pivotal role for the PD-1/PD-L1 pathway in the regulation of an autoimmune response (47). Thus, PD-L1–deficient mice develop greatly exacerbated EAE compared with control littermates, which was associated with enhanced autoantigen-specific T cell responses (34, 48). Our data extend those findings, because they

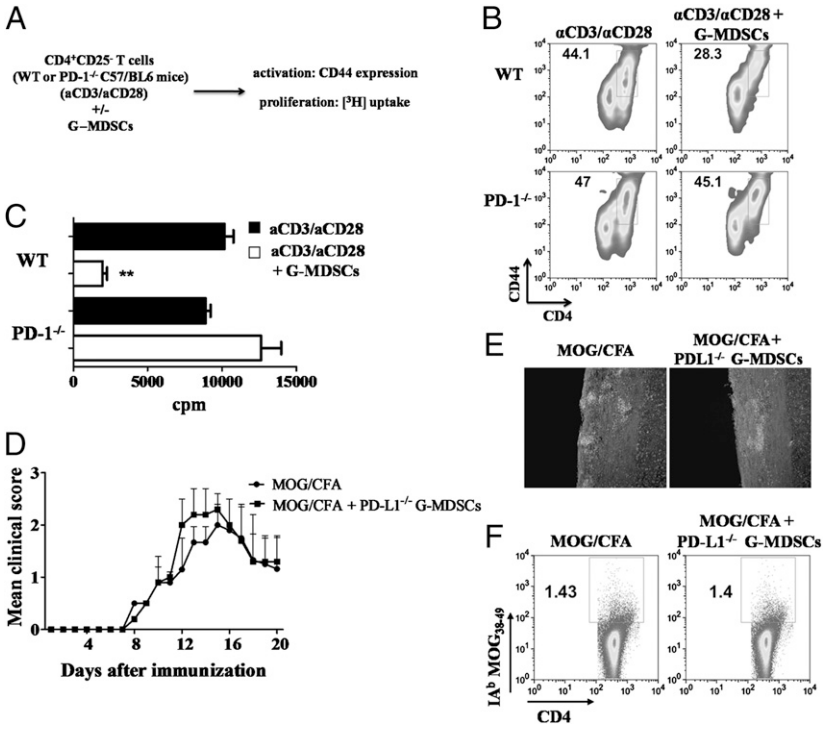

FIGURE 5. G-MDSCs suppress EAE in a PD-L1–dependent fashion both in vitro and in vivo. *A*, Schematic representation of the in vitro G-MDSC–mediated suppression assay. $CD4^+CD25^-$ T cells were sorted (purity > 99%) from spleens of naive WT or PD-$1^{-/-}$ mice and cultured (4×10^5/well) in the presence of plate-bound anti-CD3 (10 μg/ml) and anti-CD28 (1 μg/ml). Sorted G-MDSCs (purity > 95%) from spleens of MOG/CFA-immunized mice were treated with IFN-γ for 24 h and added to the cultures at a 1:1 ratio. *B*, Dot plots show CD44 expression on $CD4^+$ T cells from the indicated groups. Cells were analyzed 72 h after culture, and gates show percentages of $CD4^+CD44^+$ cells ($7AAD^-Ly6G^-CD4^+$). *C*, Cells were pulsed with 1 μCi ^{3}[H]thymidine after 72 h of culture, and incorporated thymine was measured 18 h later. Cell proliferation is expressed in cpm (mean ± SD of triplicate wells). Data in *B* and *C* are representative of three independent experiments. *D*, Mean clinical score (± SD) of EAE in mice that were adoptively transferred with PD-$L1^{-/-}$ G-MDSCs or untreated MOG/CFA immunized (control) mice (n = 6 mice/group). Cell transfer was performed as indicated in Fig. 2*A*. *E*, Representative spinal cord sections from PD-$L1^{-/-}$ G-MDSC–treated or control mice stained with Hoechst (white areas). Original magnification ×60. *F*, LNs from PD-$L1^{-/-}$ G-MDSC–treated and control mice were isolated, as described in Fig. 3*A*, and analyzed by flow cytometry for MOG_{38-49}/IA^b tetramer binding. Numbers show the frequency of $MOG_{38-49}/IA^{b+}CD4^+$ cells. Gates were set as in Fig. 3*A*. Data are representative of two independent experiments. $^{**}p = 0.003$, *t* test.

point to a PD-L1–dependent G-MDSC–mediated regulation of EAE. Furthermore, we did not detect expression of the other B7 family inhibitory molecule PD-L2 by G-MDSCs, indicating that this receptor is not involved in the G-MDSC–mediated inhibition of disease. This finding could explain the increased susceptibility of PD-$L1^{-/-}$, but not PD-$L2^{-/-}$, mice in MOG-induced EAE (34, 49). In line with our G-MDSC phenotypic data, another study demonstrated increased expression of PD-L1 in MDSCs isolated from tumor-bearing mice; however, in this report, MDSC-mediated suppression was independent of PD-L1 (14). The disparity in these results could be explained by the increased plasticity of the MDSC population and is consistent with the concept that MDSC phenotype and function would greatly depend on the microenvironmental milieu. It should be noted that, apart from

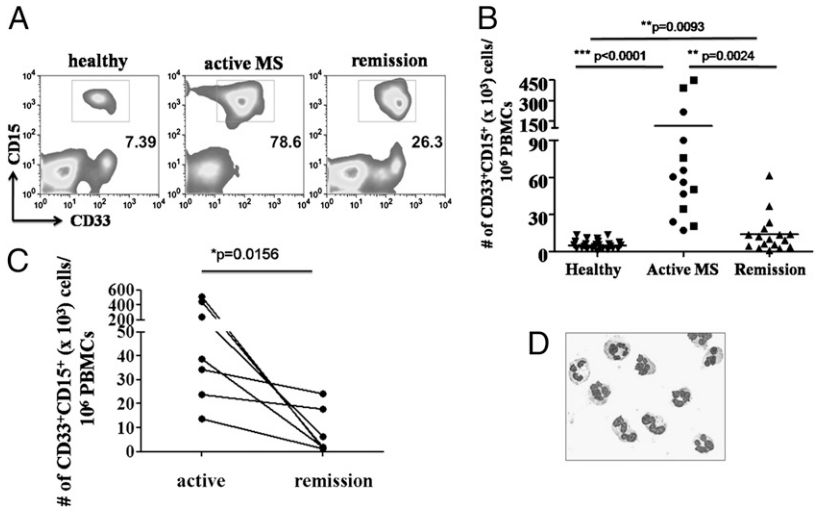

FIGURE 6. G-MDSCs are enriched in the periphery of active MS patients. Frequency (*A*) and relative numbers (*B*) of $CD33^+CD15^+$ MDSCs in the peripheral blood of MS patients with active disease (n = 14) or in remission (n = 17), as well as healthy individuals (n = 26). Gates were set on HLA-$DR^{-/low}CD14^-$ $CD33^+CD15^+$ cells. In the active MS group, ■ represents patients with first episode, whereas ● represents those in relapse. *C*, Longitudinal course of $CD33^+$ $CD15^+$ MDSCs in MS patients during active disease and 6 mo after the last relapse (remission). Each line represents an individual patient; *p* value was calculated using the Wilcoxon signed-rank test. *D*, May–Grunwald–Giemsa staining of sorted $CD33^+CD15^+$ MDSCs. Original magnification ×60.

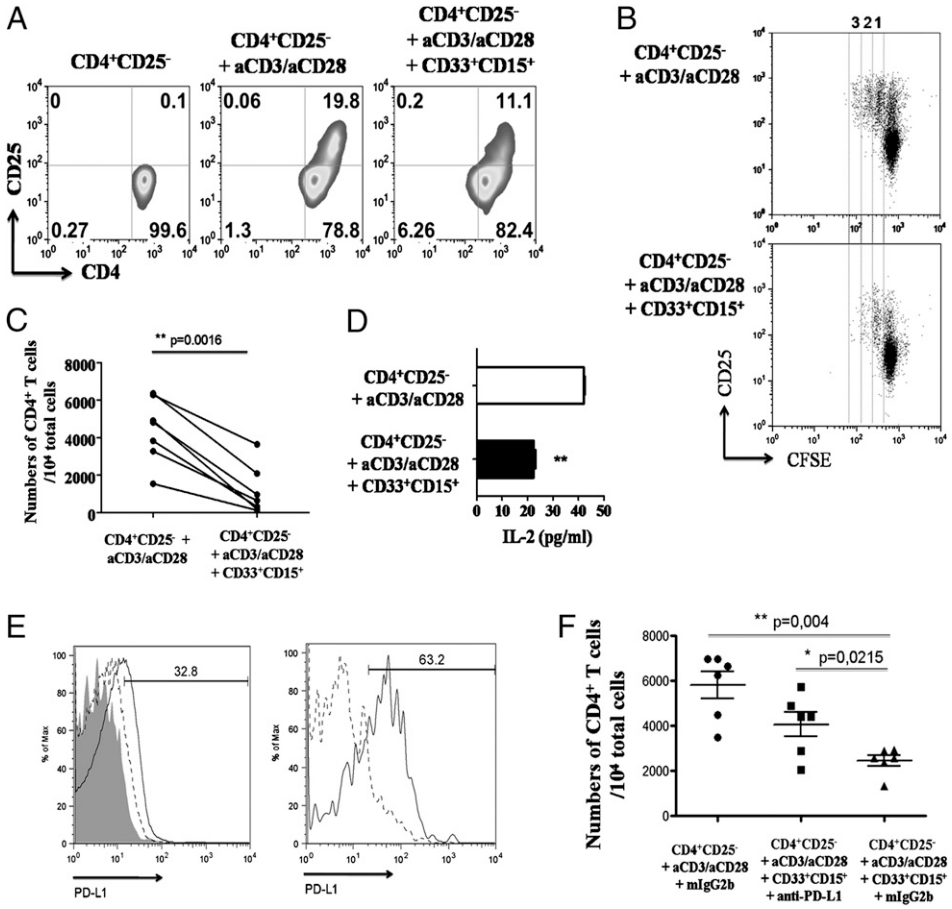

FIGURE 7. $CD33^+CD15^+$ MDSCs from active MS patients potently suppress the proliferation of autologous T cells in vitro. *A*, Sorted $CD33^+CD15^+$ MDSCs from active MS patients (purity > 95%) were cocultured with autologous $CD4^+CD25^-$ T cells (purity > 98%) with plate-bound anti-CD3 (1 μg/ml) and anti-CD28 (1 μg/ml) for 72 h. Dot plots show CD4 versus CD25 on gated viable $CD4^+$ T cells. Representative results are shown of at least three independent experiments. *B*, CFSE dilution of $CD4^+$ T cells, cultured as in *A*, in the absence (*top panel*) or presence (*bottom panel*) of MDSCs after 5 d of coculture. Numbers indicate cell divisions. *C*, $CD4^+$ T cell counts after 5 d of stimulation in the presence or absence of MDSCs. The *p* value was calculated using the *t* test. *D*, Culture supernatants were collected after 48 h and assessed for the presence of IL-2 by ELISA (mean ± SD). $^{**}p = 0.0018$, *t* test. *E*, Representative graphs for PD-L1 expression on $CD33^+CD15^+$ MDSCs from healthy individuals (dashed line) and active MS patients (solid line) (*left panel*) or untreated (dashed line) and recombinant human IFN-γ–treated (solid line; 20 ng/ml) MDSCs isolated from active MS patients (*right panel*). Shaded graph represents isotype control Ab. Data are representative of four independent experiments. *F*, Autologous $CD4^+CD25^-$ T cells from active MS patients were cocultured with $CD33^+CD15^+$ MDSCs, as described in *A*. Blocking anti-human PD-L1 (10 μg/ml) or isotype mouse IgG2b control (10 μg/ml) was added, as indicated. $CD4^+$ T cells were enumerated after 5 d of stimulation. The *p* values were calculated using the *t* test.

PD-L1, G-MDSCs from MOG/CFA-immunized mice secreted significant amounts of the immunosuppressive cytokine IL-10, indicating that several nonmutually exclusive mechanisms might contribute to the G-MDSC–mediated resolution of autoimmunity.

Our findings regarding the IFN-γ–dependent up-regulation of PD-L1 are of interest. Although IFN-γ levels are abundant both in the periphery and the target organ during the course of EAE and in MS patients, its role in the clinical outcome of the disease in both human and mice remains controversial (50–52). Our results support a regulatory role for IFN-γ in the effector phase of disease, because up-regulation of PD-L1 expression by G-MDSCs was greatly dependent on IFN-γ. This is in agreement with studies demonstrating that IFN-γ enhanced the MDSC suppressive function (53–55) and that blocking of IFN-γ totally reversed the inhibitory activity of G-MDSCs in a tumor mouse model (53). Our data reconcile findings that demonstrated exacerbation of EAE in IFN-$\gamma^{-/-}$ and IFN-$\gamma R^{-/-}$ mice or during neutralization of this cytokine (56–60). In humans, a clinical trial using IFN-γ to treat MS patients led to disease exacerbations (61); however, it was later demonstrated that IFN-γ could induce apoptosis in human oligodendrocytes, thus precipitating the autoimmune response (62, 63). In this context and based on our findings, it is worth postulating that exposure of G-MDSCs to IFN-γ during the course of the disease leads to up-regulation of PD-L1 expression, which might subsequently serve as a regulatory mechanism in controlling pathology and facilitating disease remission.

Promoting and establishing immune modulation could be a beneficial therapeutic strategy in patients with MS. Our data demonstrated that granulocytic $CD33^+CD15^+$ MDSCs were significantly enriched in the periphery of MS patients with active disease, and, importantly, they inhibited the activation and proliferation of autologous effector T cell in vitro. Consistent with the mouse data, PD-L1 expression by human $CD33^+CD15^+$ MDSCs was up-regulated in the presence of IFN-γ; however, blocking of PD-L1 expression partially restored the proliferation of autologous T cells. Further analysis of human MDSCs is required to delineate the molecules that secrete or express under autoimmune inflammatory conditions and to examine whether these molecules are involved in the MDSC potent suppressive activity. Although our study involved a relatively limited sample of MS patients, the results obtained suggested that MDSC mobilization in the peripheral blood is particularly robust at disease onset, raising the possibility

that such mobilization may contribute to clinical recovery. Of note, disease remission is more often complete after the initial attack of the disease (MS onset) than after subsequent clinical events (relapses). Because available treatments in MS are only partially effective, development of new therapies that specifically target the inflammatory autoimmune response is mandatory (64, 65).

Overall, our findings establish a critical role for G-MDSCs in the regulation of MS and provide novel insights into the mechanisms that limit inflammation during autoimmune diseases. Understanding the mechanisms that are involved in disease recovery may provide important insights into aberrant pathways that account for the chronic and progressive form of MS. The tolerogenic and immunosuppressive properties of G-MDSCs demonstrated in this study could be exploited for the development of more cell-specific–based therapies in patients with autoimmune inflammatory diseases.

Acknowledgments

We thank V. Panoutsakopoulou (Biomedical Research Foundation of the Academy of Athens, Athens, Greece) and V. Apostolopoulos (Alfred Medical Research and Education Precinct, Melbourne, VIC, Australia) for critical review of the manuscript; D. Kotzamani and K. Kanavouras (Neurology Clinic, Medical School, University of Crete) for patient care; and A. Agapaki (Biomedical Research Foundation of the Academy of Athens) for histology preparations. We also thank Z. Vlata and T. Makatounakis for technical assistance with cell sorting.

Disclosures

The authors have no financial conflicts of interest.

References

1. Steinman, L. 1996. Multiple sclerosis: a coordinated immunological attack against myelin in the central nervous system. *Cell* 85: 299–302.
2. Gold, R., C. Linington, and H. Lassmann. 2006. Understanding pathogenesis and therapy of multiple sclerosis via animal models: 70 years of merits and culprits in experimental autoimmune encephalomyelitis research. *Brain* 129: 1953–1971.
3. Diveu, C., M. J. McGeachy, and D. J. Cua. 2008. Cytokines that regulate autoimmunity. *Curr. Opin. Immunol.* 20: 663–668.
4. Sospedra, M., and R. Martin. 2005. Immunology of multiple sclerosis. *Annu. Rev. Immunol.* 23: 683–747.
5. Steinman, L. 2007. A brief history of T(H)17, the first major revision in the T(H) 1/T(H)2 hypothesis of T cell-mediated tissue damage. *Nat. Med.* 13: 139–145.
6. McGeachy, M. J., L. A. Stephens, and S. M. Anderton. 2005. Natural recovery and protection from autoimmune encephalomyelitis: contribution of CD4+CD25+ regulatory cells within the central nervous system. *J. Immunol.* 175: 3025–3032.
7. Weber, M. S., T. Prod'homme, S. Youssef, S. E. Dunn, C. D. Rundle, L. Lee, J. C. Patarroyo, O. Stüve, R. A. Sobel, L. Steinman, and S. S. Zamvil. 2007. Type II monocytes modulate T cell-mediated central nervous system autoimmune disease. *Nat. Med.* 13: 935–943.
8. Zehntner, S. P., C. Brickman, L. Bourbonnière, L. Remington, M. Caruso, and T. Owens. 2005. Neutrophils that infiltrate the central nervous system regulate T cell responses. *J. Immunol.* 174: 5124–5131.
9. Bettelli, E., M. P. Das, E. D. Howard, H. L. Weiner, R. A. Sobel, and V. K. Kuchroo. 1998. IL-10 is critical in the regulation of autoimmune encephalomyelitis as demonstrated by studies of IL-10- and IL-4-deficient and transgenic mice. *J. Immunol.* 161: 3299–3306.
10. Cua, D. J., B. Hutchins, D. M. LaFace, S. A. Stohlman, and R. L. Coffman. 2001. Central nervous system expression of IL-10 inhibits autoimmune encephalomyelitis. *J. Immunol.* 166: 602–608.
11. Gabrilovich, D. I., and S. Nagaraj. 2009. Myeloid-derived suppressor cells as regulators of the immune system. *Nat. Rev. Immunol.* 9: 162–174.
12. Gabrilovich, D. I., V. Bronte, S. H. Chen, M. P. Colombo, A. Ochoa, S. Ostrand-Rosenberg, and H. Schreiber. 2007. The terminology issue for myeloid-derived suppressor cells. *Cancer Res.* 67: 425–; author reply 426.
13. Ribechini, E., V. Greifenberg, S. Sandwick, and M. B. Lutz. 2010. Subsets, expansion and activation of myeloid-derived suppressor cells. *Med. Microbiol. Immunol.* 199: 273–281.
14. Youn, J. I., S. Nagaraj, M. Collazo, and D. I. Gabrilovich. 2008. Subsets of myeloid-derived suppressor cells in tumor-bearing mice. *J. Immunol.* 181: 5791–5802.
15. Nagaraj, S., M. Collazo, C. A. Corzo, J. I. Youn, M. Ortiz, D. Quiceno, and D. I. Gabrilovich. 2009. Regulatory myeloid suppressor cells in health and disease. *Cancer Res.* 69: 7503–7506.
16. Rabinovich, G. A., D. Gabrilovich, and E. M. Sotomayor. 2007. Immunosuppressive strategies that are mediated by tumor cells. *Annu. Rev. Immunol.* 25: 267–296.
17. Delano, M. J., P. O. Scumpia, J. S. Weinstein, D. Coco, S. Nagaraj, K. M. Kelly-Scumpia, K. A. O'Malley, J. L. Wynn, S. Antonenko, S. Z. Al-Quran, et al. 2007. MyD88-dependent expansion of an immature GR-1(+)CD11b(+) population induces T cell suppression and Th2 polarization in sepsis. *J. Exp. Med.* 204: 1463–1474.
18. Garcia, M. R., L. Ledgerwood, Y. Yang, J. Xu, G. Lal, B. Burrell, G. Ma, D. Hashimoto, Y. Li, P. Boros, et al. 2010. Monocytic suppressive cells mediate cardiovascular transplantation tolerance in mice. *J. Clin. Invest.* 120: 2486–2496.
19. Marigo, I., E. Bosio, S. Solito, C. Mesa, A. Fernandez, L. Dolcetti, S. Ugel, N. Sonda, S. Bicciato, E. Falisi, et al. 2010. Tumor-induced tolerance and immune suppression depend on the C/EBPbeta transcription factor. *Immunity* 32: 790–802.
20. Boros, P., J. C. Ochando, S. H. Chen, and J. S. Bromberg. 2010. Myeloid-derived suppressor cells: natural regulators for transplant tolerance. *Hum. Immunol.* 71: 1061–1066.
21. Marigo, I., L. Dolcetti, P. Serafini, P. Zanovello, and V. Bronte. 2008. Tumor-induced tolerance and immune suppression by myeloid derived suppressor cells. *Immunol. Rev.* 222: 162–179.
22. Serafini, P., I. Borrello, and V. Bronte. 2006. Myeloid suppressor cells in cancer: recruitment, phenotype, properties, and mechanisms of immune suppression. *Semin. Cancer Biol.* 16: 53–65.
23. Condamine, T., and D. I. Gabrilovich. 2011. Molecular mechanisms regulating myeloid-derived suppressor cell differentiation and function. *Trends Immunol.* 32: 19–25.
24. Peranzoni, E., S. Zilio, I. Marigo, L. Dolcetti, P. Zanovello, S. Mandruzzato, and V. Bronte. 2010. Myeloid-derived suppressor cell heterogeneity and subset definition. *Curr. Opin. Immunol.* 22: 238–244.
25. Youn, J. I., and D. I. Gabrilovich. 2010. The biology of myeloid-derived suppressor cells: the blessing and the curse of morphological and functional heterogeneity. *Eur. J. Immunol.* 40: 2969–2975.
26. Yin, B., G. Ma, C. Y. Yen, Z. Zhou, G. X. Wang, C. M. Divino, S. Casares, S. H. Chen, W. C. Yang, and P. Y. Pan. 2010. Myeloid-derived suppressor cells prevent type 1 diabetes in murine models. *J. Immunol.* 185: 5828–5834.
27. Haile, L. A., R. von Wasielewski, J. Gamrekelashvili, C. Kruger, O. Bachmann, A. M. Westendorf, J. Buer, R. Liblau, M. P. Manns, F. Korangy, and T. F. Greten. 2008. Myeloid-derived suppressor cells in inflammatory bowel disease: a new immunoregulatory pathway. *Gastroenterology* 135: 871–881, 881e1–5.
28. Kerr, E. C., B. J. Raveney, D. A. Copland, A. D. Dick, and L. B. Nicholson. 2008. Analysis of retinal cellular infiltrate in experimental autoimmune uveoretinitis reveals multiple regulatory cell populations. *J. Autoimmun.* 31: 354–361.
29. Marhaba, R., M. Vitacolonna, D. Hildebrand, M. Baniyash, P. Freyschmidt-Paul, and M. Zöller. 2007. The importance of myeloid-derived suppressor cells in the regulation of autoimmune effector cells by a chronic contact eczema. *J. Immunol.* 179: 5071–5081.
30. Mildner, A., M. Mack, H. Schmidt, W. Brück, M. Djukic, M. D. Zabel, A. Hille, J. Priller, and M. Prinz. 2009. CCR2+Ly-6Chi monocytes are crucial for the effector phase of autoimmunity in the central nervous system. *Brain* 132: 2487–2500.
31. King, I. L., T. L. Dickendesher, and B. M. Segal. 2009. Circulating Ly-6C+ myeloid precursors migrate to the CNS and play a pathogenic role during autoimmune demyelinating disease. *Blood* 113: 3190–3197.
32. Dardalhon, V., A. C. Anderson, J. Karman, L. Apetoh, R. Chandwaskar, D. H. Lee, M. Cornejo, N. Nishi, A. Yamauchi, F. J. Quintana, et al. 2010. Tim-3/galectin-9 pathway: regulation of Th1 immunity through promotion of CD11b+Ly-6G+ myeloid cells. *J. Immunol.* 185: 1383–1392.
33. Zhu, B., Y. Bando, S. Xiao, K. Yang, A. C. Anderson, V. K. Kuchroo, and S. J. Khoury. 2007. CD11b+Ly-6C(hi) suppressive monocytes in experimental autoimmune encephalomyelitis. *J. Immunol.* 179: 5228–5237.
34. Latchman, Y. E., S. C. Liang, Y. Wu, T. Chernova, R. A. Sobel, M. Klemm, V. K. Kuchroo, G. J. Freeman, and A. H. Sharpe. 2004. PD-L1-deficient mice show that PD-L1 on T cells, antigen-presenting cells, and host tissues negatively regulates T cells. *Proc. Natl. Acad. Sci. USA* 101: 10691–10696.
35. Nagaraj, S., A. G. Schrum, H. I. Cho, E. Celis, and D. I. Gabrilovich. 2010. Mechanism of T cell tolerance induced by myeloid-derived suppressor cells. *J. Immunol.* 184: 3106–3116.
36. Keir, M. E., M. J. Butte, G. J. Freeman, and A. H. Sharpe. 2008. PD-1 and its ligands in tolerance and immunity. *Annu. Rev. Immunol.* 26: 677–704.
37. Almand, B., J. I. Clark, E. Nikitina, J. van Beynen, N. R. English, S. C. Knight, D. P. Carbone, and D. I. Gabrilovich. 2001. Increased production of immature myeloid cells in cancer patients: a mechanism of immunosuppression in cancer. *J. Immunol.* 166: 678–689.
38. Schmielau, J., and O. J. Finn. 2001. Activated granulocytes and granulocyte-derived hydrogen peroxide are the underlying mechanism of suppression of t-cell function in advanced cancer patients. *Cancer Res.* 61: 4756–4760.
39. Fridlender, Z. G., J. Sun, S. Kim, V. Kapoor, G. Cheng, L. Ling, G. S. Worthen, and S. M. Albelda. 2009. Polarization of tumor-associated neutrophil phenotype by TGF-beta: "N1" versus "N2" TAN. *Cancer Cell* 16: 183–194.
40. Tsuda, Y., H. Takahashi, M. Kobayashi, T. Hanafusa, D. N. Herndon, and F. Suzuki. 2004. Three different neutrophil subsets exhibited in mice with different susceptibilities to infection by methicillin-resistant *Staphylococcus aureus*. *Immunity* 21: 215–226.
41. Zhang, X., L. Majlessi, E. Deriaud, C. Leclerc, and R. Lo-Man. 2009. Coactivation of Syk kinase and MyD88 adaptor protein pathways by bacteria promotes regulatory properties of neutrophils. *Immunity* 31: 761–771.
42. Haverkamp, J. M., S. A. Crist, B. D. Elzey, C. Cimen, and T. L. Ratliff. 2011. In vivo suppressive function of myeloid-derived suppressor cells is limited to the inflammatory site. *Eur. J. Immunol.* 41: 749–759.

43. Tu, S., G. Bhagat, G. Cui, S. Takaishi, E. A. Kurt-Jones, B. Rickman, K. S. Betz, M. Penz-Oesterreicher, O. Bjorkdahl, J. G. Fox, and T. C. Wang. 2008. Overexpression of interleukin-1beta induces gastric inflammation and cancer and mobilizes myeloid-derived suppressor cells in mice. *Cancer Cell* 14: 408–419.
44. Bunt, S. K., P. Sinha, V. K. Clements, J. Leips, and S. Ostrand-Rosenberg. 2006. Inflammation induces myeloid-derived suppressor cells that facilitate tumor progression. *J. Immunol*. 176: 284–290.
45. Song, X., Y. Krelin, T. Dvorkin, O. Bjorkdahl, S. Segal, C. A. Dinarello, E. Voronov, and R. N. Apte. 2005. CD11b+/Gr-1+ immature myeloid cells mediate suppression of T cells in mice bearing tumors of IL-1beta-secreting cells. *J. Immunol.* 175: 8200–8208.
46. Li, L., L. Huang, A. L. Vergis, H. Ye, A. Bajwa, V. Narayan, R. M. Strieter, D. L. Rosin, and M. D. Okusa. 2010. IL-17 produced by neutrophils regulates IFN-gamma-mediated neutrophil migration in mouse kidney ischemia-reperfusion injury. *J. Clin. Invest.* 120: 331–342.
47. Francisco, L. M., P. T. Sage, and A. H. Sharpe. 2010. The PD-1 pathway in tolerance and autoimmunity. *Immunol. Rev.* 236: 219–242.
48. Keir, M. E., S. C. Liang, I. Guleria, Y. E. Latchman, A. Qipo, L. A. Albacker, M. Koulmanda, G. J. Freeman, M. H. Sayegh, and A. H. Sharpe. 2006. Tissue expression of PD-L1 mediates peripheral T cell tolerance. *J. Exp. Med.* 203: 883–895.
49. Carter, L. L., M. W. Leach, M. L. Azoitei, J. Cui, J. W. Pelker, J. Jussif, S. Benoit, G. Ireland, D. Luxenberg, G. R. Askew, et al. 2007. PD-1/PD-L1, but not PD-1/PD-L2, interactions regulate the severity of experimental autoimmune encephalomyelitis. *J. Neuroimmunol.* 182: 124–134.
50. Lees, J. R., P. T. Golumbek, J. Sim, D. Dorsey, and J. H. Russell. 2008. Regional CNS responses to IFN-gamma determine lesion localization patterns during EAE pathogenesis. *J. Exp. Med.* 205: 2633–2642.
51. Axtell, R. C., B. A. de Jong, K. Boniface, L. F. van der Voort, R. Bhat, P. De Sarno, R. Naves, M. Han, F. Zhong, J. G. Castellanos, et al. 2010. T helper type 1 and 17 cells determine efficacy of interferon-beta in multiple sclerosis and experimental encephalomyelitis. *Nat. Med.* 16: 406–412.
52. Stromnes, I. M., L. M. Cerretti, D. Liggitt, R. A. Harris, and J. M. Goverman. 2008. Differential regulation of central nervous system autoimmunity by T(H)1 and T(H)17 cells. *Nat. Med.* 14: 337–342.
53. Movahedi, K., M. Guilliams, J. Van den Bossche, R. Van den Bergh, C. Gysemans, A. Beschin, P. De Baetselier, and J. A. Van Ginderachter. 2008. Identification of discrete tumor-induced myeloid-derived suppressor cell subpopulations with distinct T cell-suppressive activity. *Blood* 111: 4233–4244.
54. Huang, B., P. Y. Pan, Q. Li, A. I. Sato, D. E. Levy, J. Bromberg, C. M. Divino, and S. H. Chen. 2006. Gr-1+CD115+ immature myeloid suppressor cells mediate the development of tumor-induced T regulatory cells and T-cell anergy in tumor-bearing host. *Cancer Res.* 66: 1123–1131.
55. Gallina, G., L. Dolcetti, P. Serafini, C. De Santo, I. Marigo, M. P. Colombo, G. Basso, F. Brombacher, I. Borrello, P. Zanovello, et al. 2006. Tumors induce a subset of inflammatory monocytes with immunosuppressive activity on CD8+ T cells. *J. Clin. Invest.* 116: 2777–2790.
56. Willenborg, D. O., S. Fordham, C. C. Bernard, W. B. Cowden, and I. A. Ramshaw. 1996. IFN-gamma plays a critical down-regulatory role in the induction and effector phase of myelin oligodendrocyte glycoprotein-induced autoimmune encephalomyelitis. *J. Immunol.* 157: 3223–3227.
57. Chu, C. Q., S. Wittmer, and D. K. Dalton. 2000. Failure to suppress the expansion of the activated CD4 T cell population in interferon gamma-deficient mice leads to exacerbation of experimental autoimmune encephalomyelitis. *J. Exp. Med.* 192: 123–128.
58. Heremans, H., C. Dillen, M. Groenen, E. Martens, and A. Billiau. 1996. Chronic relapsing experimental autoimmune encephalomyelitis (CREAE) in mice: enhancement by monoclonal antibodies against interferon-gamma. *Eur. J. Immunol.* 26: 2393–2398.
59. Lublin, F. D., R. L. Knobler, B. Kalman, M. Goldhaber, J. Marini, M. Perrault, C. D'Imperio, J. Joseph, S. S. Alkan, and R. Korngold. 1993. Monoclonal anti-gamma interferon antibodies enhance experimental allergic encephalomyelitis. *Autoimmunity* 16: 267–274.
60. Ferber, I. A., S. Brocke, C. Taylor-Edwards, W. Ridgway, C. Dinisco, L. Steinman, D. Dalton, and C. G. Fathman. 1996. Mice with a disrupted IFN-gamma gene are susceptible to the induction of experimental autoimmune encephalomyelitis (EAE). *J. Immunol.* 156: 5–7.
61. Panitch, H. S., R. L. Hirsch, A. S. Haley, and K. P. Johnson. 1987. Exacerbations of multiple sclerosis in patients treated with gamma interferon. *Lancet* 1: 893–895.
62. Pouly, S., B. Becher, M. Blain, and J. P. Antel. 2000. Interferon-gamma modulates human oligodendrocyte susceptibility to Fas-mediated apoptosis. *J. Neuropathol. Exp. Neurol.* 59: 280–286.
63. Vartanian, T., Y. Li, M. Zhao, and K. Stefansson. 1995. Interferon-gamma-induced oligodendrocyte cell death: implications for the pathogenesis of multiple sclerosis. *Mol. Med.* 1: 732–743.
64. Feldmann, M., and L. Steinman. 2005. Design of effective immunotherapy for human autoimmunity. *Nature* 435: 612–619.
65. Hohlfeld, R., and H. Wekerle. 2004. Autoimmune concepts of multiple sclerosis as a basis for selective immunotherapy: from pipe dreams to (therapeutic) pipelines. *Proc. Natl. Acad. Sci. USA* 101(Suppl. 2): 14599–14606.

Corrections

Ioannou, M., T. Alissafi, I. Lazaridis, G. Deraos, J. Matsoukas, A. Gravanis, V. Mastorodemos, A. Plaitakis, A. Sharpe, D. Boumpas, and P. Verginis. 2012. Crucial role of granulocytic myeloid-derived suppressor cells in the regulation of central nervous system autoimmune disease. *J. Immunol.* 188: 1136–1146.

In Fig. 1B, there is no legend for the *x*-axis on the FACS plots. The legend for the *x*-axis is CD11b.

In Fig. 4F, the titles for the second and third FACS plots were incorrectly attributed. The second FACS plot represents CD86 and the third FACS plot represents CD80.

www.jimmunol.org/cgi/doi/10.4049/jimmunol.1390073